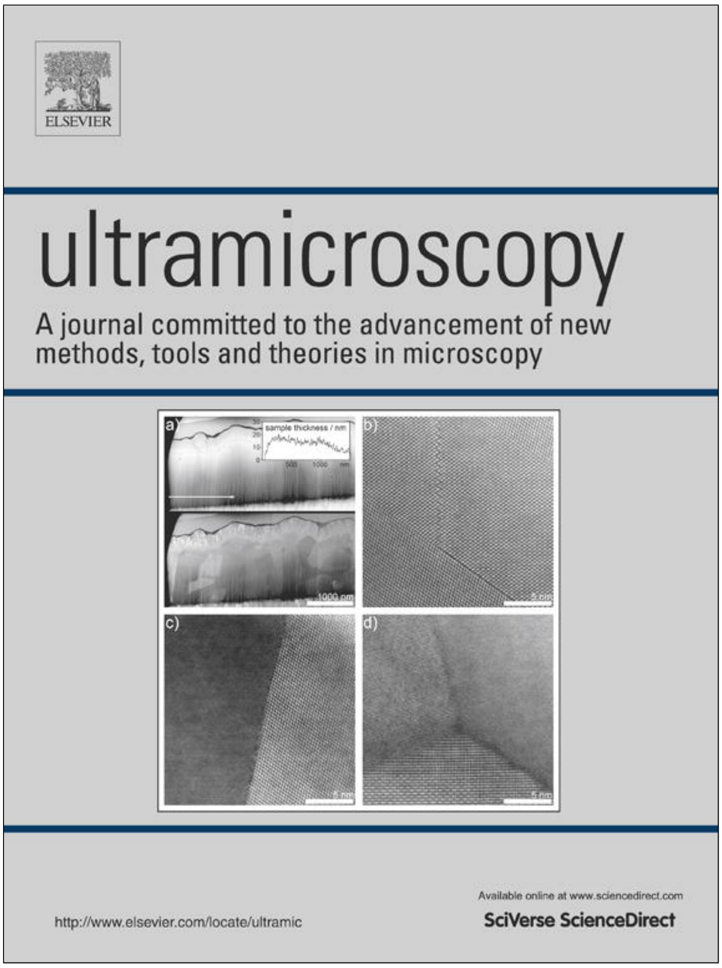
ELSEVIER
ultramicroscopy
A journal committed to the advancement of new methods, tools and theories in microscopy
http://www.elsevier.com/locate/ultramic
Available online at www.sciencedirect.com
SciVerse ScienceDirect

Ultramicroscopy 118 (2012) 21–25

Contents lists available at SciVerse ScienceDirect

Ultramicroscopy

journal homepage: www.elsevier.com/locate/ultramic

Improvement of the accuracy of phase observation by modification of phase-shifting electron holography

Takahiro Suzuki [a], Shinji Aizawa [a], Toshiaki Tanigaki [a], Keishin Ota [b,*], Tsuyoshi Matsuda [c], Akira Tonomura [a,d,e]

[a] Advanced Science Institute, RIKEN, Hirosawa 2–1, Wako, Saitama 351–0198, Japan
[b] Microphase Co., Ltd., Onigakubo 1147–9, Tsukuba, Ibaragi 300–2651, Japan
[c] Japan Science and Technology Agency, Kawaguchi-shi, Saitama 332–0012, Japan
[d] Okinawa Institute of Science and Technology, Graduate University, Kunigami, Okinawa 904–0495, Japan
[e] Central Research Laboratory, Hitachi, Ltd., Hatoyama, Saitama 350–0395, Japan

ARTICLE INFO

Article history:
Received 27 January 2012
Received in revised form
1 April 2012
Accepted 28 April 2012
Available online 11 May 2012

Keywords:
Electron holography
Phase-shifting
Phase reconstruction

ABSTRACT

We found that the accuracy of the phase observation in phase-shifting electron holography is strongly restricted by time variations of mean intensity and contrast of the holograms. A modified method was developed for correcting these variations. Experimental results demonstrated that the modification enabled us to acquire a large number of holograms, and as a result, the accuracy of the phase observation has been improved by a factor of 5.

1. Introduction

Electron holography [1] is a powerful method to accurately observe phase images of an electron wave transmitted through phase objects, such as electric fields [2], magnetic fields [3], or thin specimens. The resultant accuracy of the phase (here we mean the standard deviation from the total image area of the resultant phase image) is directly related to the observation limit of electron holography. Improving the accuracy is thought to be an important work.

Many efforts have been made to improve the accuracy of the phase observations: increasing the signal to noise ratio by acquiring high electron density to achieve a high contrast hologram [4] or by using multiple holograms [5,6], reducing the artifact errors due to phase calculations by improving the phase analysis algorithm [7,8], improving the Fourier-transform phase reconstruction method [8], and developing phase-shifting methods [9–11].

We are particularly interested in a phase-shifting method because it has a high potential to achieve a high accuracy of the phase observation with less loss of the spatial resolution. The phase-shifting method was developed in optical interferometry [12], and then modified and applied to electron holography [9,10]. In the method, a number of holograms with different initial phases are acquired by slightly changing the angle of incident electron beam, and then the phase image of the specimen is computed from the intensity data of these holograms. It has been shown that the accuracy of the obtained phase image can be greatly improved in principle by increasing the number of the input holograms. The best phase accuracy reported so far was 0.02 rad (about $2\pi/300$ rad) [13], where 24 holograms were acquired and used.

Increasing the number of the input holograms will lead to a long total exposure time, during which the interference conditions including mean intensity (proportional to the electron counts in the image recording plane) and contrast of the hologram fringes should be kept unchanged. In practice, however, mean intensity and contrast usually vary with time. For example, the fluctuation of the current density of electron gun [14] directly causes mean intensity fluctuation, and the time variations of the electron source position and the biprism position [5] cause contrast variation. In addition, since the incident beam needs to be continuously tilted in order to change the initial phase of each hologram in the phase-shifting method, mean intensity and contrast certainly vary according to the tilt angle. If the conventional phase analysis algorithms are used without considering these time variations, calculation errors as artifacts will appear in the resultant phase image, reducing the final accuracy of the phase observation.

In this paper, a method is reported for correcting mean intensity and contrast variations in phase-shifting hologram series. The effect of the correction is then demonstrated on real data.

* Corresponding author. Tel.: +81 298483322; fax: +81 298483323.
E-mail address: ota@microphase.co.jp (K. Ota).

0304-3991/$ - see front matter © 2012 Elsevier B.V. All rights reserved.
http://dx.doi.org/10.1016/j.ultramic.2012.04.007

2. Modification of phase-shifting electron holography

The phase-shifting method is based on obtaining and calculating a series of holograms with different initial phases. The intensity distribution of the n-th hologram $I\_n(x,y)(1 \leqq n \leqq N)$ can be described by the following formula.

$$I\_n(x,y) = B\_n(1 + A(x,y)^2 + 2A(x,y) \cdot C\_n \cdot \cos\left(\frac{2\pi x}{T_x} + \frac{2\pi y}{T_y} + \phi(x,y) - \phi_0\_n\right), \quad (1)$$

where, $A(x,y)$and $\phi(x,y)$ denote the amplitude and the phase distribution of the object wave to be observed, T_x and T_y denote the interference fringe pitches in x and y directions, and B_n and C_n denote the mean intensity and contrast, respectively. Term ϕ_0_n is the initial phase of the n-th hologram, which bears resemblance with the lateral phase of the hologram.

First, we describe how to correct the time variation of the mean intensity term B_n. In order to evaluate the actual mean-intensity in each hologram, a small local rectangular area in the hologram is selected as a monitor area that contains no (or very little) contribution from the specimen. Under these conditions, the amplitude term $A(x,y)$ can be considered as unity, and the actual mean intensity term B_n in each hologram can be obtained by averaging the intensity over all the area. Then the mean intensity variation is corrected by dividing the original intensity data $I\_n(x,y)$ by the obtained value B_n, i.e., $Ib\_n(x,y) = I\_n(x,y)/B\_n$. Thus a new series of mean-intensity-corrected hologram data $Ib\_n(x,y)$ are obtained, which have a constant mean intensity.

Next, we describe how to correct the time variation in the contrast C_n. We note that the contrast correction is applicable only for phase object or weak-amplitude object observations. Under these conditions, the amplitude term $A(x,y)$ can be considered as unity. The two-dimensional Fourier transform of the mean-intensity-corrected intensity distribution data in the monitor area is performed for each hologram, and then a center-band and two equivalent side bands are obtained in the complex Fourier space [10]. Because the contrast term C_n is proportional to the amplitude of side-band peak, the contrast C_n of each hologram is measured from the peak value of the side-band of the hologram. Then the contrast variation is corrected by calculating the formula $Ic\_n(x,y) = \{Ib\_n(x,y)\text{-}2\}/C\_n$. Thus a new series of contrast-corrected hologram data $Ic\_n(x,y)$ are obtained, which have both a constant mean intensity and a constant contrast.

After these correction procedures, the phase distribution of the object is computed by using the phase analysis algorithms proposed by Ru et al. [10].

3. Experiments and results

In order to evaluate and demonstrate effects of the modified phase-shifting method, we performed two experiments: first, a vacuum field without any specimen, and second, an electric field near a charged Si-tip, were observed. Both specimens can be considered as pure phase objects. In the first experiment, because no specimen information is included in holograms, the resultant phase distribution is expected to be perfectly smooth and flat. If any undulation distribution is observed, the undulated phase values can be directly interpreted as the observation errors, which contain the contributions from the following tree kinds of major error sources: 1) non-ideal beam-illumination conditions, 2) distortion in the fiber optics of the CCD camera, and 3) ill-condition of the phase-calculation algorithms which is discussed in this paper. For simplicity here, we assume that the former two errors are smaller than the last one, and so we consider that the resultant errors are mainly caused from the calculation algorithms. By comparing the error levels with mean-intensity corrections and/or contrast corrections to those without any correction, we can check the correction performances.

Holograms were formed by using Hitachi HF-3000X and HF- 3300X transmission electron microscopes (Hitachi High-Technologies Co., Japan) equipped with a cold field-emission gun operated at 300 kV. A double-biprism method [15] was used to form the holograms and to reduce the Fresnel diffraction at the electron biprism. A charge-coupled device camera (ORIUS^{TM} SC200, Gatan Inc., USA) with 2048×2048 pixels was used with a binning factor of 4 to acquire the holograms. The hologram image width was 1600 nm related to the object plane. Because a hologram image is sampled by 512 pixels, the spatial resolution in the reconstructed phase image was limited to 3.125 nm. The initial phase of each hologram was changed by tilting the incident beam [9]. The total amount of the beam tilt was about 0.0001 rad and the total amount of the initial phase change was about 6π rad (three fringe cycles). The fringe spacing was 24 pixels/fringe related to the CCD plane and 32 nm/fringe related to the object plane. The exposure time of each hologram was 10 s, 160 holograms with different initial phases were obtained, and the total hologram recording time including the beam tilt adjusting time and the data transfer time was 1 h. The phase analysis computations were performed by using the "Phase Analysis Software" developed by Microphase Co., Ltd (Tsukuba, Japan) based on phase-shifting algorithms [10].

One of the hologram images is shown in Fig. 1(a), and the time variations of mean intensity and contrast of these 160 holograms were measured and shown in Fig. 1(b) and (c), respectively. From the graphs of Fig. 1(b) and (c), we can see that the ratio of the

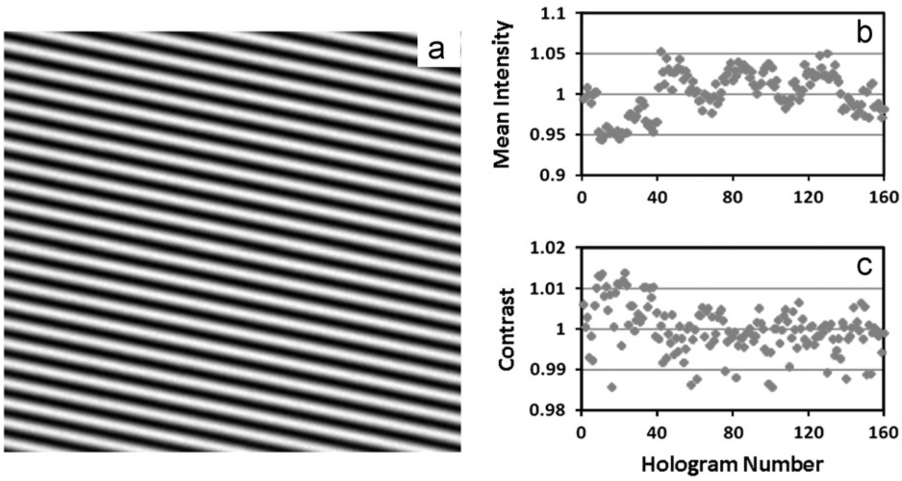

Fig. 1. (a) One of the acquired 160 hologram images, (b) the line profile of the mean intensity variation, (c) the contrast variation measured from these 160 holograms.

variation of the mean-intensity is much larger than that of the contrast, indicating that the mean-intensity correction is more important than the contrast correction. To show these correction effects quantitatively, the phase distributions reconstructed from the hologram data with and without corrections were obtained and shown in Fig. 2 with blown-up gray-scale levels. Fig. 2(a) shows the phase image reconstructed without any correction, Fig. 2(b) shows that with only mean-intensity correction, and Fig. 2(c) shows that with both mean intensity and contrast corrections. Because the double-biprism system was used, Fresnel fringes due to biprism diffraction, which usually have undulated fringe contrast, are hardly recognized in Fig. 1(a), and the phase errors caused from the Fresnel fringes are also not recognized in Fig. 2. Line profiles corresponding to these reconstructed phase distributions along the lines (as marked in Fig. 2) perpendicular (right side) and parallel (left side) to the interference fringes are shown in Fig. 3. In the case that no corrections were performed as shown in Fig. 3(a), the resultant phase profile perpendicular to the fringes has much larger periodical errors than that parallel to the fringes. This kind of artifact errors is usually observed when the interference conditions, such as mean intensity, contrast, initial phase, fringe pitch, and Fresnel diffraction at the electron biprism, did not meet to the conditions required from the conventional phase-shifting method. The pattern of the artifact errors is known to be similar to the original hologram fringe pattern, so that a periodical fringe-like error pattern is usually observed. In the case that no corrections were performed, a phase accuracy, defined by the standard deviation of the phase values over the entire area of the reconstructed phase image [5,7], was ± 0.02132 (about $2\pi/300$ rad). Fig. 3(b) shows the results obtained with only mean-intensity correction. The errors in the perpendicular to the fringes markedly decreased. The phase accuracy with mean-intensity correction was ± 0.00464 (about $2\pi/1300$ rad), which is 4.5 times better than those obtained without corrections.

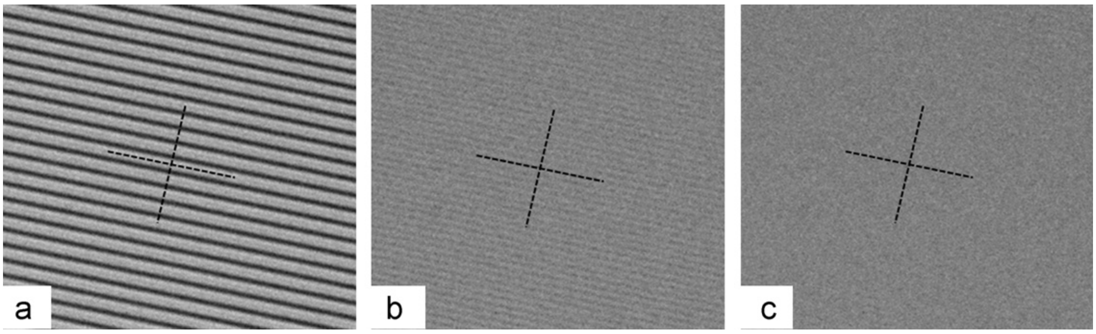

Fig. 2. Reconstructed phase images with blown-up gray levels. (a) No correction was performed, (b) only mean intensity correction was performed, and (c) both mean intensity and contrast corrections were performed. Lines drawn in the pictures denote the directions of line profiles shown in Fig. 3.

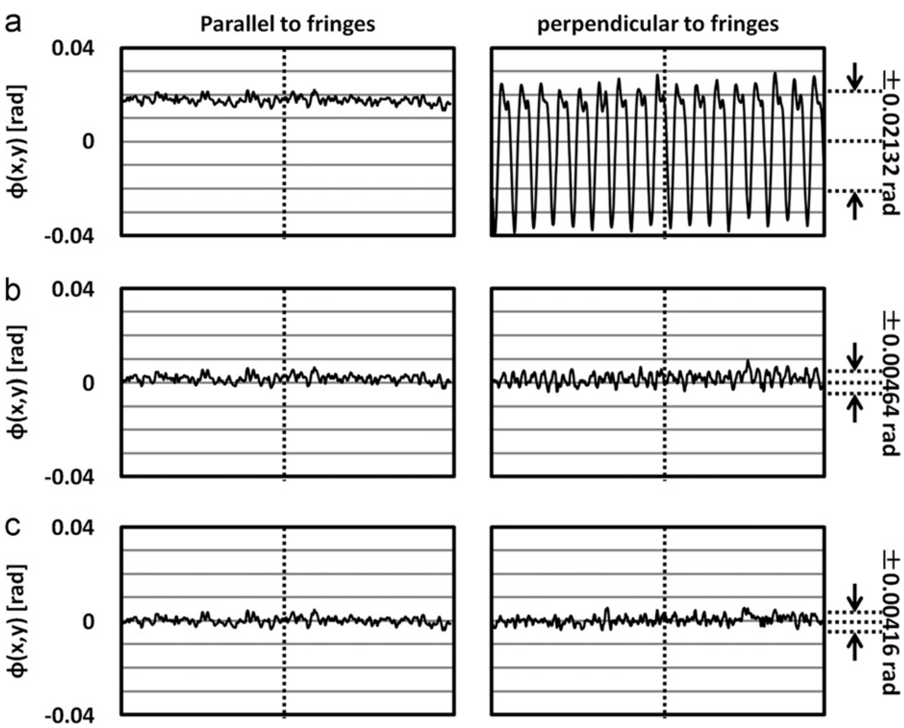

Fig. 3. Line profiles of reconstructed phase images in vacuum area. Data for parallel to fringes was shown on the left side and data for perpendicular to fringes was shown on the right side. (a) Data without mean-intensity and contrast corrections. In the perpendicular direction, periodical artifact appeared. In the parallel direction, phase value deviates from 0 rad due to the artifact in the perpendicular direction. The phase noise, defined by standard deviation of the resultant errors over the entire area of the reconstructed phase image, was ± 0.02132 rad. (b) Data with only mean-intensity correction. The phase noise was ± 0.00464 rad in the perpendicular direction, whereas in the parallel direction, phase value was approached 0 rad. (c) Data with both mean-intensity and contrast correction. The artifact was removed. The phase noise was the same for both directions, i.e., 0.00416 rad.

Fig. 3(c) shows the results obtained with both mean intensity and contrast corrections. The periodical artifact errors in the phase profile perpendicular to the fringes almost vanished. The phase accuracy was 0.00416 ($2\pi/1500$ rad), which is almost 5 times better than that without corrections.

In the specimen-less experiment, we have confirmed that the correction procedures basically reduced the artifact errors and improved the accuracy of the phase observation. In order to demonstrate a good performance for practical specimen, we observed an electric field near a charged Si-tip; this is also a pure phase object.

Fig. 4 shows schematic diagram of the Si-tip specimen setting. In order to reduce phase changes due to a contact potential, a voltage of -2.6 V was applied to the Si-tip.

The experimental conditions were the same as described above, except that the total number of the acquired holograms was increased to 600 and the fringe pitch was 8 pixels (40 nm).

Fig. 5(a) shows a hologram of the specimen, in which the Si-tip is located at the upper left corner of the hologram. A monitor area denoted by a red rectangle was selected and used to measure the mean intensity B_n and contrast C_n variations, with the results of $B\_n = 720 \pm 70$ electrons/pixel and $C\_n = 20 \pm 1.3\%$.

Fig. 5(b) shows the reconstructed phase image with a color map and Fig. 5(c) shows a line profile along the white line AB in Fig. 5(b). An exponentially decreasing phase profile outside the Si-tip region was observed, which is proportional to the electric field from the charged Si-tip. An exponential fitting [16] was performed on the experimental phase profile and the obtained fitted line profile in blue is shown in the upper graph of Fig. 5(d). The difference between the experimental curve and fitted curve shown in the bottom graph of Fig. 5(d) is considered as phase error ϕ_{Err}. The phase accuracy defined by the standard deviation of these errors [5,7] was 0.00145 ($2\pi/4340$ rad).

4. Discussions

We have shown that the modification algorithm described in this paper improved the phase accuracy by a factor of 5. Although the algorithm was quite simple, it was effective for reducing periodic artifact errors due to the variations in mean intensity and contrast.

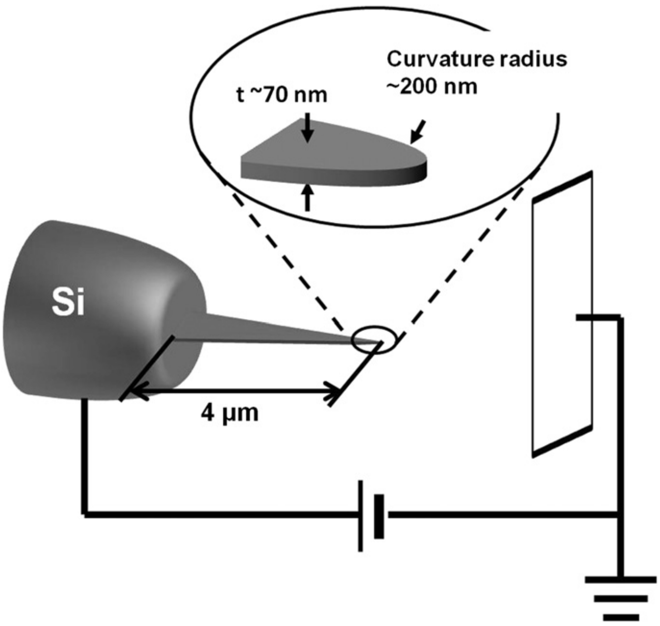

Fig. 4. Experimental setting of Si-tip. The shape of Si-tip was 4 µm in length, 70 nm in thickness, and 200 nm in curvature radius. To reduce the phase shift due to contact potential, a voltage of -2.6 V was applied to the Si-tip.

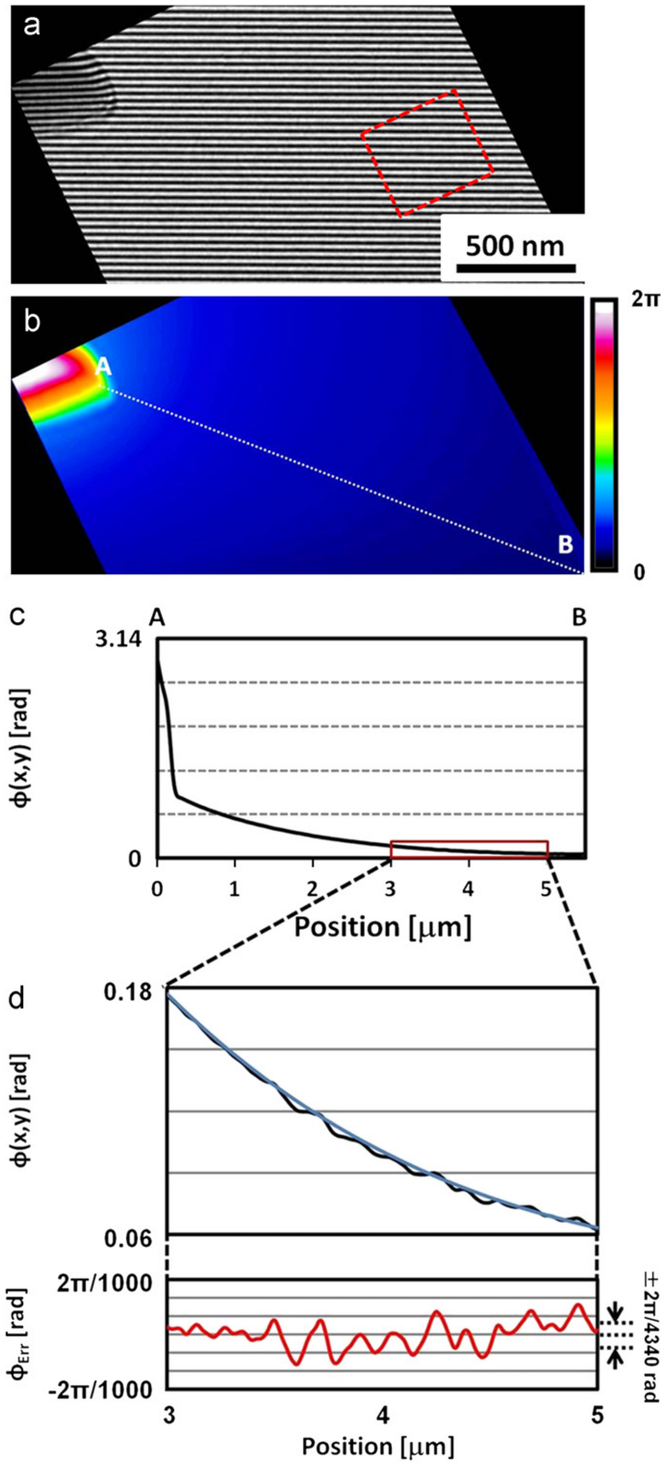

Fig. 5. Hologram and reconstructed phase image of near the Si-tip with mean-intensity and contrast corrections. The phase shift of reconstructed image is averaged over a 7×7 pixels area. (a) Hologram. The Si-tip locates at the upper left corner. Red rectangle area is used to measure the mean-intensity and contrast variations. (b) Reconstructed phase image with a color map. (c) The line profile along the line AB denoted in Fig. 5(b). (d) Upper graph shows the line profile and fitting curve for the position between 3 and 5 µm for the origin. Lower graph shows profile of the phase errors ϕ_{Err}, defined by the difference between experimental data and the fitting curve data. (For interpretation of the references to color in this figure legend, the reader is referred to the web version of this article.)

However, there are still important problems remaining in the modified method. In experiments described in this paper, only phase objects were used as specimens, so that a monitor area can be selected to measure the mean-intensity and contrast variations. In most cases, however, specimens to be observed may have an amplitude distribution. If the amplitude distributes over all area of the holograms, further improvements of the modified method are necessary, because the selection of a monitor area will become much difficult.

5. Conclusion

In the phase-shifting method using a large number of holograms, we found that the time variations of mean intensity and contrast in the holograms were a significant cause of artifacts (calculation error) in reconstructed phase image, and that the artifact was a major factor for reducing the accuracy of the phase result. We developed a modified method to reduce artifacts due to those variations. The mean intensity and contrast values were measured from each obtained hologram data, and the variation values were replaced by average values to rebuild a new series of hologram data with variation-free mean intensity and contrast values. By applying the conventional phase-shifting algorithms to the corrected hologram data, the artifact in the reconstructed phase image was greatly removed, and the phase accuracy was improved by a factor of 5. We believe that this method will lead to realize a much better observation method of electron phase shifts within $2\pi/1000$ rad.

Acknowledgements

The authors gratefully acknowledge Dr Hideki Ichinose and Dr Yoshimasa A. Ono for valuable discussions. This research was supported by the grant from the Japan Society for the Promotion of Science (JSPS) through the "Funding Program for World-Leading Innovative R&D on Science and Technology (FIRST Program)," initiated by the Council for Science and Technology Policy (CSTP).

References

[1] A. Tonomura, Electron-holographic interference microscopy, Advances in Physics 41 (1992) 59–103.
[2] D. Shindo, Y. Murakami, Electron holography study of electric field variations, Journal of Electron Microscopy 60 (2011) S225–S237.
[3] D. Shindo, Y. Murakami, Electron holography of magnetic materials, Journal of Physics D: Applied Physics 41 (2008) 183002. (21 pp).
[4] H. Lichte, Performance limits of electron holography, Ultramicroscopy 108 (2008) 256–262.
[5] E. Voelkl, D. Tang, Approaching routine $2\pi/1000$ phase resolution for off-axis type holography, Ultramicroscopy 110 (2010) 447–459.
[6] K. Yamamoto, T. Hirayama, T. Tanji, M. Hibino, Evaluation of high-precision phase-shifting electron holography by using hologram simulation, Surface and Interface Analysis 35 (2003) 60–65.
[7] H. Lichte, D. Geiger, A. Harscher, E. Heindl, M. Lehmann, D. Malamidis, A. Orchowski, W.-D. Rau, Artifact in electron holography, Ultramicroscopy 64 (1996) 67–77.
[8] M. Lehmann, H. Lichte, Tutorial on off-axis electron holography, Microscopy and Microanalysis 8 (2002) 447–466.
[9] Q. Ru, J. Endo, T. Tanji, A. Tonomura, Phase-shifting electron holography by beam tilting, Applied Physics Letters 59 (1991) 2372–2374.
[10] Q. Ru, G. Lai, K. Aoyama, J. Endo, A. Tonomura, Principle and application of phase-shifting electron holography, Ultramicroscopy 55 (1994) 209–220.
[11] T. Fujita, K. Yamamoto, M.R. McCartney, D.J. Smith, Reconstruction technique for off-axis electron holography using coarse fringes, Ultramicroscopy 106 (2006) 486–491.
[12] J.H. Bruning, D.R. Herriott, J.E. Gallagher, D.P. Rosenfeld, A.D. White, D.J. Brangaccio, Digital wavefront measuring interferometer for testing optical surfaces and lenses, Applied Optics 13 (1974) 2693–2703.
[13] K. Yamamoto, I. Kawajiri, T. Tanji, M. Hibino, T. Hirayama, High precision phase-shifting electron holography, Journal of Electron Microscopy 49 (2000) 31–39.
[14] S. Yamamoto, N. Saitou, S. Fukuhara, Field emission current instability induced by migrating atoms on W(310) surface, Surface Science 71 (1978) 191–198.
[15] K. Harada, A. Tonomura, Y. Togawa, T. Akashi, T. Matsuda, Double-biprism electron interferometry, Applied Physics Letters 84 (2004) 3229–3231.
[16] G. Matteucci, G.F. Missiroli, M. Muccini, G. Pozzi, Electron holography in the study of the electrostatic field: the case of charged microtips, Ultramicroscopy 45 (1992) 77–83.